Optical Phase Locking by Local Oscillator Phase Dithering

Frank Herzog, *Member, IEEE*, Klaus Kudielka, Daniel Erni, *Member, IEEE*, and Werner Bächtold, *Fellow, IEEE*

Abstract—A new type of optical phase-locked loop (OPLL), called the dither loop, is mathematically analyzed. The dither loop extracts a phase-error signal by applying a small phase distur- bance to the local oscillator laser, and synchronously demodulating the resulting power fluctuation in the output signal of the receiver. The dither loop is superior to other OPLL designs, because it does not need the transmission of a residual carrier, it employs a 180°/3-dB hybrid, an ac-coupled front end, and it accepts a large variety of input signals. Furthermore, in a dither loop, the amount of power which is fed to the phase-locking branch can be adaptively controlled within the receiver. The analysis first focuses on an expression for the phase detector gain in a dither loop. Using a linearized model, the phase-error variance due to phase dithering, white frequency noise induced phase noise and shot noise is evaluated. A simplified expression for the power penalty generated by the phase dither signal is presented. In a more com- plex calculation, the overall power penalty due to phase dithering and the residual phase error is found. This allows us to synthesize a design rule for dither loops with optimum performance measures. The design rule determines all relevant system parameters, based on specified values of the system bit rate, the laser linewidth, the photodiode responsivity and the required bit-error rate.

Index Terms—Homodyne detection, optical phase-locked loops (OPLLs), satellite communication.

I. INTRODUCTION

IN THE optical domain, coherent detection has several fundamental advantages over direct detection. Coherent receivers, operating in shot-noise-limited conditions, can ap- proach the theoretical sensitivity limit of 9 photons/bit (for a bit-error rate (BER) of 10^{-9}), while direct detection receivers usually suffer from considerable power penalties referred to the quantum limit of direct detection of 10 photons/bit [1]–[5]. For space communication applications, coherent receivers are less susceptible to background illumination from the sun, due to an increased mode and wavelength selectivity [6]. As a further advantage, coherent detection offers the use of angular modu- lation schemes and subcarrier multiplexing techniques [7]–[9]. To harness these benefits, system designers have to deal with a

significantly increased technological effort compared to direct detection receivers.

It has been theoretically shown that, in coherent optical de- tection, an inherent 3-dB power penalty exists for heterodyne receivers compared to homodyne receivers [1], [10], [11]. For this reason, homodyne reception is the technology of choice for an optical transmission system with maximum sensitivity. Ho- modyning requires an optical phase-locked loop (OPLL), for which several designs are known. The most common are the balanced loop [12]–[15] and the Costas or decision-driven loop [16]–[20]. Other loop types use synchronization bits for phase locking [21], or additional phase modulation of the transmitter (TX) signal [22], [23]. This paper is concerned with the dither loop phase-locking scheme [9], [24], [25], which operates with the synchronous demodulation of a small phase disturbance ap- plied to the the local oscillator (LO) laser.

The reason for this variety of OPLL designs lies in various limitations of optical network elements. First, 90° couplers with asymmetric coupling ratio (e.g., 90% in-phase, 10% quadra- ture), as they are needed in Costas loops, are made of lossy combinations of beam splitters and polarization controllers [26]–[30]. Second, the transmission of a residual carrier, as it is used in balanced loops, is a disadvantage especially in combination with an optical booster amplifier [31]. In addition, the residual-carrier transmission requires a dc-coupled front end [32]. Other OPLL designs, which circumvent both the 90° coupler as well as the residual-carrier transmission, perform extensive pre- and post-processing on the user signal [33]. From a system engineer's perspective, an ideal homodyne receiver design should have the following characteristics:

- it employs a symmetrical 180°/3-dB coupler;
- it does not require the transmission of a residual carrier;
- the front end can be ac-coupled;
- analog and digital transmission at user-specified data rates is supported;
- no extensive data pre- or postprocessing is required;
- the amount of signal power which is used for phase locking is a system variable, preferably within the receiver.

Of all known OPLL types, the dither loop receiver is the only design which fulfills all the above mentioned constraints. The only limitation is a constant envelope of the transmitted user signal.

In this work, we present a mathematical analysis of the dither loop for the first time. Noise effects on the phase-error vari- ance are treated in a similar way as in [12] and [16] for other OPLL types. A major distinction lies in the fact that, in a dither loop, the phase-locking mechanism (i.e., the dither signal) can be considered as an internal noise source of the feedback system.
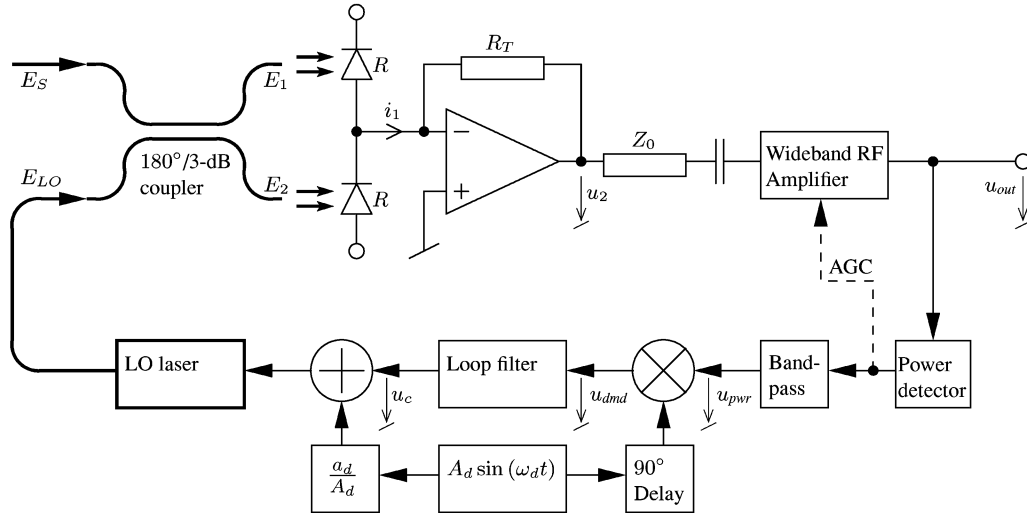
Fig. 1. Schematic overview of the dither loop receiver. Thick lines indicate optical components or signals.

By calculating the influence of all relevant noise sources on the phase-error variance and the BER, the dither loop can be optimized for maximum performance.

The remainder of this paper is organized as follows. A general description of the dither loop receiver is given in Section II. The mathematical analysis of the phase error extraction, and the calculation of the phase detector gain, is presented in Section III. Section IV focuses on the effects of phase dithering, phase noise and shot noise on the phase-locking performance. Likewise, in Section V, the noise-induced degradation of the communication performance is analyzed. The findings from the previous sections are used in Section VI to develop a dither loop design rule. To demonstrate the design rule, examples are given for various system specifications.

II. SYSTEM OVERVIEW

The proposed dither loop is shown in Fig. 1. The receiver branch consists of the local oscillator laser and an optical hybrid, followed by a balanced detector front end. The transimpedance amplifier provides impedance matching, and a RF amplifier boosts the received signal to the desired output level. A dc-coupling from the photodiodes to the system output is not required for loop operation. The balanced detector front end reduces loss by using both branches of the coupler, and it provides LO intensity noise suppression [34].

In the phase-locking branch, a small deterministic phase disturbance, called the dither signal, is applied to the LO phase. The dither signal propagates through the receiver and can be measured at the system output as a signal power fluctuation. After bandpass filtering and synchronous demodulation, a measure for the incident phase error can be extracted. A 90° phase shift must be introduced in the reference input of the demodulation multiplier. This is because of the frequency-to-phase conversion of the dither signal in the LO laser. As in any PLL, the loop filter determines the dynamics of the feedback loop.

For the dither loop to operate properly, the dither frequency has to be chosen much larger (e.g., by a factor of 10) than the natural frequency of the loop. This way, the feedback loop can

not (and shall not) suppress the dither signal. The dither signal is present in the receiver output and reduces the signal-to-noise ratio (SNR). The amount of SNR reduction can be considered as the power penalty that has to be paid for phase locking (see Section V-A).

As a second requirement for successful loop operation, the average power of the transmitted user signal has to be on a constant level (i.e., a constant-envelope signal). For PSK modulated binary data, this condition is inherently satisfied. For the transmission of analog signals, the constant average power can be achieved by using frequency modulated electrical subcarriers. It is believed that the constant average power requirement is a minor limitation of the dither loop compared to its advantages, which comprise the use of a 180°/3-dB coupler, an ac-coupled front end and a residual-carrier free transmission. Furthermore, in a dither loop, the amount of power which is fed into the phase-locking branch can be adaptively controlled according to the receiving conditions.

III. PHASE-ERROR EXTRACTION

This section contains the mathematical analysis of the phase error extraction in the dither loop receiver. The analysis starts with the definition of the received and the LO optical fields

$$E_S = \sqrt{P_S} \cdot e^{j\phi_S} \tag{1a}$$

$$E_{\mathrm{LO}} = \sqrt{P_{\mathrm{LO}}} \cdot e^{j\phi_{\mathrm{LO}}} \tag{1b}$$

where P_S and P_{LO} denote the power and ϕ_S and ϕ_{LO} the phase of the complex envelope. The optical coupler, being a symmetrical 180°/3-dB device, generates the sum and the difference of its input fields

$$E_1 = \frac{1}{\sqrt{2}}(E_S + E_{\mathrm{LO}}) \tag{2a}$$

$$E_2 = \frac{1}{\sqrt{2}}(E_S - E_{\mathrm{LO}}). \tag{2b}$$

Illuminating the surface of a photodiode with an optical field E will lead to a current of

$$i_{pd} = R \cdot |E|^2 \quad (3)$$

flowing through the diode, where R is the responsivity in A/W. Plugging (1) and (2) into (3), and solving for the total current flowing into the transimpedance amplifier, yields

$$i_1 = i_{pd1} - i_{pd2} = 2R\sqrt{P_S P_{LO}} \cdot \cos(\phi_S - \phi_{LO}). \quad (4)$$

Shot noise has been neglected here. It will be introduced in Section IV-C. The transimpedance amplifier, the matching network and the RF amplifier provide gain factors of R_T (in Ω), 1/2, and G_{RF} (scalar), respectively. Thus, the output signal of the receiver amounts to

$$u_{out} = -G_{RF} R_T R \sqrt{P_S P_{LO}} \cdot \cos(\phi_S - \phi_{LO})$$
$$= -U_0 \cos(\phi_S - \phi_{LO}). \quad (5)$$

The expression

$$U_0 = G_{RF} R_T R \sqrt{P_S P_{LO}} \quad (6)$$

is the amplitude of the output signal in V. In a real world receiver, an automatic gain control (AGC) circuit for G_{RF} would ensure that U_0 stays independent of the received power P_S.

So far, the dither loop operates like a balanced loop, e.g., as in [12]. The main difference lies in the definition of the phase expressions ϕ_S and ϕ_{LO}

$$\phi_S(t) = \frac{\pi}{2} + \frac{\pi}{2}d(t) + \phi_{nS}(t) \quad (7a)$$

$$\phi_{LO}(t) = G_{vco} \int_{-\infty}^t (u_c(\tau) + a_d \sin(\omega_d \tau))d\tau + \phi_{nLO}(t)$$
$$= G_{vco} \int_{-\infty}^t u_c(\tau)d\tau - \phi_d \cos(\omega_d t) + \phi_{nLO}(t). \quad (7b)$$

The first expression in (7a), $\pi/2$, anticipates the quadrature phase lock behavior of the PLL, i.e., in the locked condition, a 90° phase difference exists between the two lasers [12], [35]. The data signal $d(t)$ takes values in $\{-1, 1\}$ for "zero" and "one" bits. It can be seen in the coefficient $\pi/2$ of $d(t)$ that the TX laser is fully modulated, i.e., no residual-carrier transmission takes place. The phase noise process of the TX laser is denoted by $\phi_{nS}(t)$. In (7b), G_{vco} is the frequency tuning sensitivity of the LO laser in rad/s/V, $u_c(t)$ refers to the loop filter output voltage, and a_d and ω_d are the dither voltage amplitude and angular frequency (the normal dither frequency will be denoted by $f_d = \omega_d/2\pi$). The resulting phase amplitude of the dither signal is called

$$\phi_d = \frac{a_d G_{vco}}{\omega_d} \quad (8)$$

in rad, and $\phi_{nLO}(t)$ denotes the phase noise process of the LO laser. For further calculation, it is convenient to use the following notation:

$$\phi_E(t) = \phi_e(t) + \phi_d \cos(\omega_d t) \quad (9a)$$
$$\phi_e(t) = \phi_n(t) - \phi_c(t)$$
$$= \phi_n(t) - G_{vco} \int_{-\infty}^t u_c(\tau)d\tau \quad (9b)$$
$$\phi_n(t) = \phi_{nS}(t) - \phi_{nLO}(t). \quad (9c)$$

The total phase error $\phi_E(t)$ consists of the residual phase error $\phi_e(t)$ and the phase dither signal. The LO phase due to the loop filter output is written as $\phi_c(t)$, and $\phi_n(t)$ denotes the combined phase noise process of the two lasers. Using (7) and (9) in (5) yields for the system output, after transformations

$$u_{out}(t) = U_0 d(t) \cos \phi_E(t). \quad (10)$$

As it can be expected, a phase error of zero maximizes the amplitude of the output signal. The polarity of the output is determined by the data signal $d(t)$. A direct measure for the incident phase error is not present in (10), because the $\cos \phi_E(t)$ expression decreases for positive as well as negative deviations of $\phi_E(t)$ from the desired value of zero.

The phase-locking branch of the receiver first measures the power of the output signal

$$u_{pwr}(t) = G_{pwr} \frac{u_{out}^2(t)}{Z_0} = C_1 u_{out}^2(t) \quad (11)$$

where G_{pwr} denotes the sensitivity of the power detector in V/W, and Z_0 is the impedance of the output transmission line. For the rest of this analysis, C_1 replaces G_{pwr}/Z_0 for brevity. Evaluating (10) and (9a) in (11) leads to

$$u_{pwr}(t) = \frac{U_0^2 C_1}{2}(1 + \cos(2\phi_e(t))\cos(2\phi_d \cos(\omega_d t))$$
$$- \sin(2\phi_e(t))\sin(2\phi_d \cos(\omega_d t))). \quad (12)$$

For the $\cos(\cos(\cdot))$ and $\sin(\cos(\cdot))$ expressions in (12), the following series expansion can be used (e.g., from [36]):

$$\cos(z \cos \theta) = J_0(z) + 2\sum_{k=1}^{\infty}(-1)^k J_{2k}(z) \cos(2k\theta) \quad (13a)$$

$$\sin(z \cos \theta) = 2\sum_{k=0}^{\infty}(-1)^k J_{2k+1}(z) \cos((2k+1)\theta) \quad (13b)$$

where $J_n(\cdot)$ denotes the Bessel function of the first kind of order n. With (13), the power detector output (12) becomes

$$u_{pwr}(t) = \frac{U_0^2 C_1}{2}(1 + \cos(2\phi_e(t))(J_0(2\phi_d)$$
$$- 2J_2(2\phi_d)\cos(2\omega_d t)$$
$$+ 2J_4(2\phi_d)\cos(4\omega_d t) - \dots)$$
$$- \sin(2\phi_e(t))(2J_1(2\phi_d)\cos(\omega_d t)$$
$$- 2J_3(2\phi_d)\cos(3\omega_d t)$$
$$+ 2J_5(2\phi_d)\cos(5\omega_d t) - \dots)). \quad (14)$$

The dc terms in (14) are removed by the bandpass filter which follows the power detector. Furthermore, it can be reasoned that, for small arguments z, $J_1(z)$ exceeds $J_n(z)$ by far for $n > 1, n \in \mathbf{N}$. The relevant power detector output signal then amounts to

$$u_{\mathrm{pwr}}(t) = -U_0^2 C_1 J_1(2\phi_d) \cos(\omega_d t) \sin(2\phi_e(t)). \quad (15)$$

For mathematical simplicity, the bandpass filter will not be included in the calculation. To have a negligible effect on the noise performance of the OPLL, its transfer function has to be flat (in frequency and phase) across a frequency range of approximately $f_d \pm B_n$, where B_n denotes the loop noise bandwidth (introduced in Section IV).

Synchronous demodulation occurs in a multiplier with a reference voltage K_{dmd}. The reference voltage is necessary to have reasonable output units, i.e., V instead of V^2. Feeding the multiplier with (15) and the phase shifted dither signal, $-A_d \cos(\omega_d t)$, results in

$$u_{\mathrm{dmd}}(t) = \frac{U_0^2 C_1 A_d}{K_{\mathrm{dmd}}} \cdot J_1(2\phi_d) \cos^2(\omega_d t) \sin(2\phi_e(t)). \quad (16)$$

The $\cos^2(\cdot)$ expression contains a dc-term of 1/2 and a component at twice the dither frequency, which will be suppressed by the closed-loop transfer function. Thus, the multiplier output becomes

$$u_{\mathrm{dmd}}(t) = \frac{U_0^2 C_1 C_2}{2} \cdot J_1(2\phi_d) \sin(2\phi_e(t)) \quad (17)$$

where C_2 replaces A_d/K_{dmd} for brevity. Further simplification can be made using the approximations for small arguments z

$$J_\nu(z) \approx \frac{(z/2)^\nu}{\Gamma(\nu+1)} \quad (18)$$

from [36], and

$$\sin(z) \approx z \quad (19)$$

which follows from the Taylor series expansion of the sine function. In (18), $\Gamma(\cdot)$ denotes the Gamma function, related to the factorial by $\Gamma(n) = (n-1)!$ if n is an integer. Finally, with (18) and (19) in (17), a measure for the residual phase error $\phi_e(t)$ has been extracted

$$u_{\mathrm{dmd}}(t) = U_0^2 \phi_d C_1 C_2 \cdot \phi_e(t) = K_{\mathrm{PD}} \cdot \phi_e(t)$$
$$= \frac{G_{\mathrm{RF}}^2 R_T^2 R^2 P_S P_{\mathrm{LO}} a_d G_{\mathrm{vco}} G_{\mathrm{pwr}} A_d}{\omega_d Z_0 K_{\mathrm{dmd}}} \cdot \phi_e(t). \quad (20)$$

The fraction on the right side of (20) can be considered as the phase detector gain K_{PD} of the OPLL in V/rad. The various parameters of (20) are summarized in Table I, with feasible values for a real world receiver.

TABLE I
FEASIBLE PARAMETER VALUES FOR A REAL WORLD DITHER LOOP RECEIVER

Parameter	Symbol	Units	Example value
Received power	P_S	dBm	-50
LO power	P_{LO}	dBm	10
Photodiode responsivity	R	A/W	0.64
Transimpedance	R_T	Ω	1000
RF amplifier gain	G_{RF}	scalar	11
Output voltage	U_0	V	$7.1 \cdot 10^{-2}$
Dither voltage amplitude	a_d	V	$7 \cdot 10^{-3}$
Dither frequency	ω_d	rad/s	$2\pi \cdot 10^5$
VCO sensitivity	G_{vco}	rad/s/V	$2\pi \cdot 10^6$
Dither phase amplitude	ϕ_d	deg	4
Power detector gain	G_{pwr}	V/W	$1.43 \cdot 10^5$
Transmission line impedance	Z_0	Ω	50
G_{pwr}/Z_0	C_1	V^{-1}	2865
Amplitude for demodulation	A_d	V	10
Multiplier reference voltage	K_{dmd}	V	10
A_d/K_{dmd}	C_2	scalar	1
Phase detector gain	K_{PD}	V/rad	1

In a dither loop, the phase detector is a distributed device, extending over the entire system. Phase sensing occurs in the photodiodes, but since no optical carrier has been transmitted, the receiver output does not contain a direct phase-error signal. By phase dithering and synchronous demodulation, it is determined in which direction the phase error $\phi_e(t)$ decreases, and the LO phase is tracked accordingly. In other publications, this phase locking strategy is called "phase synchronization by maximizing base-band signal power" [24]. Similar approaches have been used in heterodyne DPSK systems for IF tracking [37], or in direct detection systems for active delay line stabilization [38].

IV. NOISE IN A DITHER LOOP

Noise affects a coherent receiver in two ways. Shot noise directly flows into the data-detection branch, generating bit errors at low levels of the SNR. Phase noise, and other noise signals which flow into the phase-locking branch, lead to a residual phase error. The phase error inevitably reduces the signal amplitude, and therefore deteriorates the SNR. In this section, expressions for the phase-error variance due to the major noise sources will be calculated.

To ease the mathematics, the phase-error variance is analyzed by means of a linearized model of the dither loop as depicted in Fig. 2. For the linearized model to be accurate, the following conditions have to be satisfied.

- The total phase error $\phi_E(t)$ should remain small, e.g., the total phase error standard deviation σ_E should not exceed $10°$.
- The dither frequency f_d is much larger than the natural frequency of the loop f_n, e.g., by a factor of 10.
- The bandpass filter has a negligible effect on the closed-loop transfer function of the OPLL. This implies that the bandpass filter transfer function is flat in frequency and phase across a frequency range of approximately $f_d \pm B_n$, where B_n denotes the loop noise bandwidth.

It will be shown in Section VI how to calculate the total phase error standard deviation σ_E, so that the first condition can be verified mathematically. The second condition is a pure matter
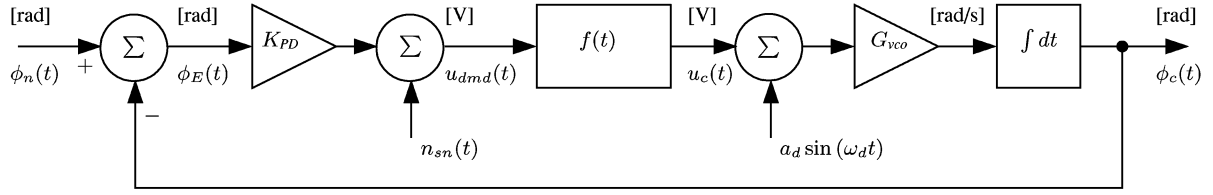
Fig. 2. Linearized dither loop model.

of choice, provided that the bandwidth of the LO frequency tuning input reaches up to f_d (if not, an external phase modulator has to be used). For the third condition, it can be reasoned that $f_d > B_n$, since $f_d \gg f_n$ and B_n depends on f_n by (24c) given later. Therefore, it is usually possible to design a first-order bandpass filter that provides the desired dc and high frequency filtering, without affecting the closed-loop transfer function.

With the linearized model, the closed-loop transfer function of the loop can be computed

$$H(s) = \frac{\mathcal{L}\{\phi_c(t)\}}{\mathcal{L}\{\phi_n(t)\}} = \frac{s^{-1}G_{\text{loop}}F(s)}{1 + s^{-1}G_{\text{loop}}F(s)}. \quad (21)$$

Likewise, the error transfer function amounts to

$$1 - H(s) = \frac{\mathcal{L}\{\phi_E(t)\}}{\mathcal{L}\{\phi_n(t)\}} = \frac{1}{1 + s^{-1}G_{\text{loop}}F(s)}. \quad (22)$$

In (21) and (22), $G_{\text{loop}} = K_{\text{PD}}G_{\text{vco}}$ denotes the overall loop gain with units of s^{-1}, and $\mathcal{L}\{\cdot\}$ is the Laplace transform. To obtain analytical expressions for the phase-error variance, it is necessary to define the loop filter transfer function $F(s)$. In PLL theory, a common choice is a first order active filter with a transfer function of

$$F(s) = \frac{s\tau_2 + 1}{s\tau_1} \quad (23)$$

with the two time constants τ_1 and τ_2 [12], [16], [35], [39]. This filter provides proportional/integral control, which can be seen in the infinite gain at zero frequency. With (23) in (21), the following parameters are defined:

$$2\pi f_n = \omega_n = \sqrt{\frac{G_{\text{loop}}}{\tau_1}} \quad (24a)$$

$$\zeta = \frac{\tau_2}{2}\sqrt{\frac{G_{\text{loop}}}{\tau_1}} = \frac{\omega_n \tau_2}{2} \quad (24b)$$

$$B_n = \int_0^\infty |H(f)|^2 df = \pi f_n\left(\zeta + \frac{1}{4\zeta}\right). \quad (24c)$$

In control theory, f_n, ζ and B_n are called the natural frequency, the damping factor and the noise bandwidth of the loop. In the following, the noise performance of the dither loop is analyzed by means of the linearized model of Fig. 2 and the loop filter transfer function (23).

A. Phase Dithering

The dither signal is not noise in a strict sense, due to its deterministic nature. Furthermore, it is intentionally applied to the loop. Still, for mathematical coherence, it is convenient to treat the dither signal like an internal noise source of the receiver. Since, by requirement, the dither frequency f_d is much larger than the natural frequency f_n, the system can be considered to be in open loop condition concerning dither signal injection.

Generally written, the variance of the phase-error signal is defined as

$$\sigma_E^2 = \text{E}\left[\phi_E^2(t)\right] - \text{E}^2[\phi_E(t)] \quad (25)$$

where $\text{E}[\cdot]$ denotes the expected value. With all noise sources except phase dithering switched off, (9a) for the total phase error amounts to

$$\phi_E(t) = \phi_d \cos(\omega_d t). \quad (26)$$

Evaluation of (26) in (25) yields

$$\sigma_{E,\text{dither}}^2 = \frac{\phi_d^2}{2} = \frac{1}{2}\cdot\left(\frac{a_d G_{\text{vco}}}{\omega_d}\right)^2 \quad (27)$$

which is the phase-error variance due to LO phase dithering, solely dependent on the phase dither amplitude ϕ_d.

B. Phase Noise

A dither loop processes phase noise in the same way as other OPLL types [12], [16], [40]. The evaluation is therefore not repeated here. It is only recalled that the phase noise process $\phi_n(t)$ has a single-sided power spectral density (PSD) of

$$S_{\text{pn}}(f) = \frac{2\Delta\nu}{\pi f^2} \quad (28)$$

where $\Delta\nu$ denotes the 3 dB linewidth of the lasers. The PSD of (28) is valid for white frequency noise induced phase noise. The phase-error variance due to phase noise can be calculated through

$$\sigma_{E,\text{pn}}^2 = \int_0^\infty S_{\text{pn}}(f)|1 - H(f)|^2 df. \quad (29)$$

According to (22), $1 - H(f)$ is the error transfer function of the loop. Using the loop filter (23), and evaluating (28) in (29), results in

$$\sigma_{E,\text{pn}}^2 = \frac{3\pi\Delta\nu}{4B_n} \tag{30}$$

where a critically damped loop ($\zeta = 1/\sqrt{2}$) has been assumed. Equation (30) describes the phase-error variance in a dither loop due to laser phase noise, as a function of the laser linewidth $\Delta\nu$ and the loop noise bandwidth B_n.

C. Shot Noise

When taking shot noise into account, the receiver output (10) becomes

$$u_{\text{out}}(t) = U_0 d(t) \cos\phi_E(t) - R_T G_{\text{RF}}/2 \cdot n(t) \tag{31}$$

where $n(t)$ denotes the combined shot noise process of the two photodiodes with a one-sided PSD of

$$S_n(f) = 2qRP_{\text{LO}} \tag{32}$$

in A^2/Hz. The shot noise signal flows through the power detector, bandpass filter and demodulator into the loop filter. The shot noise signal at the loop filter input will be denoted by $n_{\text{sn}}(t)$ with an associated PSD of $S_{\text{sn}}(f)$. The following calculation focuses on an expression for $S_{\text{sn}}(f)$. It is kept in mind that the shot noise PSD $S_n(f)$ is limited by the front end cut-off frequency B_{RF}.

When fed with (31), the power detector output (11) yields

$$u_{\text{pwr}}(t) = C_1 (U_0 d(t) \cos(\phi_E) - R_T G_{\text{RF}}/2 \cdot n(t))^2$$
$$= C_1 \left(U_0^2 d^2(t) \cos^2\phi_E(t) \right.$$
$$- \underbrace{U_0 R_T G_{\text{RF}} d(t) n(t) \cos\phi_E(t)}_{(\text{signal}\times\text{noise})}$$
$$+ \left. \underbrace{(R_T G_{\text{RF}}/2)^2 \cdot n^2(t)}_{(\text{noise}\times\text{noise})} \right). \tag{33}$$

The first expression in (33) is further processed to extract the phase error, as developed in Section III. The second expression will be called the signal × noise beat note, and the third expression is the noise × noise beat note.

1) Signal × Noise Beat Note: To calculate the PSD of the signal×noise beat note, the following approximations are made:

$$\cos\phi_E(t) \approx 1 \tag{34a}$$
$$S_{[d(t)n(t)]}(f) \approx S_n(f) \tag{34b}$$
$$S_{[n(t)\cos(\omega_d t)]}(f) \approx S_n(f)/2. \tag{34c}$$

The first line holds true when the total phase error remains small. This is assumed throughout this paper. To justify (34b), it has to be kept in mind that $d(t)$ is a random binary nonreturn to zero (NRZ) signal which takes only values in $\{-1, 1\}$. According to [41], the PSD of $d(t)$ computes to

$$S_d(f) = T_b \cdot \frac{\sin(\pi f T_b)}{\pi f T_b} \tag{35}$$

where T_b is the bit interval in seconds. The PSD $S_d(f)$ has its main power content in frequencies below the system bit rate $R_b = 1/T_b$. The convolution of $S_d(f)$ with $S_n(f)$ yields approximately $S_n(f)$ as long as $R_b \leq B_{\text{RF}}$. The third approximation, (34c), states that a frequency shift does not affect the power spectral density of a white noise process, except for a multiplicative factor of 1/2. This becomes apparent when bearing in mind that the power spectrum of $\cos(\cdot)$ is a delta function with area 1/2. Applying (34) to the signal × noise beat note, its PSD can be written as

$$S_{\text{sn1}}(f) = \frac{(U_0 C_1 C_2 R_T G_{\text{RF}})^2}{2} \cdot S_n(f). \tag{36}$$

The C_2 term in (36) is introduced during synchronous demodulation, as shown in the evaluation of K_{PD} in Section III [(16)–(17)]. The signal × noise beat note with a PSD of (36) flows into the OPLL and possibly affects its performance.

2) Noise × Noise Beat Note: With the shot noise process $n(t)$ being a stationary normal process, it is known from [42] that the PSD of $n^2(t)$ can be calculated through

$$S_{[n^2(t)]}(f) = R_n^2(0)\delta(f) + 2S_n(f) \star S_n(f) \tag{37}$$

where $R_n(\tau)$ denotes the autocorrelation function of $n(t)$, and "$\star$" is the convolution operator. The $R_n^2(0)$ term in (37) is equal to the square of the total power of the shot noise process $n(t)$, i.e., $(S_n B_{\text{RF}})^2$. The convolution in (37) yields a ramp with a maximum value of $S_n^2 B_{\text{RF}}$ at $f = 0$ and a minimum value of 0 at $f = 2B_{\text{RF}}$. Thus, the PSD of the squared shot noise process, $n^2(t)$, can be written as

$$S_{[n^2(t)]}(f) = S_n^2 \begin{cases} B_{\text{RF}}^2 \delta(f) + 2B_{\text{RF}} - f, & f \leq 2B_{\text{RF}} \\ 0, & \text{else} \end{cases} \tag{38}$$

with units of A^4/Hz. The bandpass filter removes the dc term and high frequency parts of the ramp function. Furthermore, it can be reasoned that $B_{\text{RF}} \gg f_d$, so that $2B_{\text{RF}} - f \approx B_{\text{RF}}$ for frequencies around f_d. Thus, the PSD of the noise × noise beat note amounts to

$$S_{\text{sn2}}(f) = \left(\frac{C_1 C_2}{\sqrt{2}} \left(\frac{R_T G_{\text{RF}}}{2} \right)^2 \right)^2 \cdot 2S_n^2(f) B_{\text{RF}} \tag{39}$$

where, as for the signal × noise beat note, the $C_2/\sqrt{2}$ term has been introduced during synchronous demodulation.
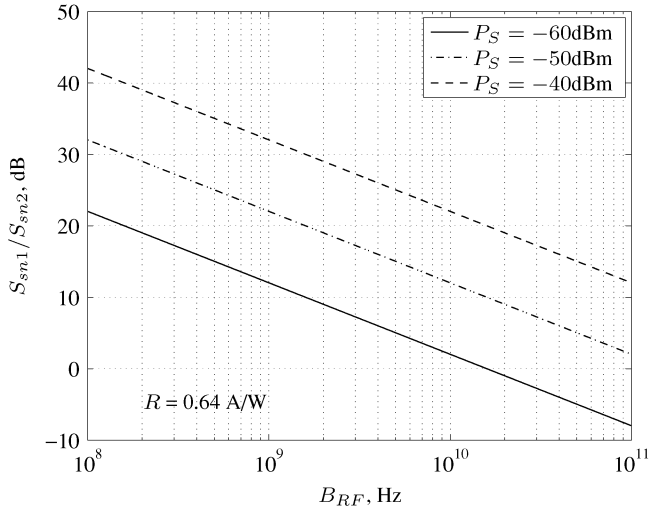
Fig. 3. Shot noise power ratio $S_{\mathrm{sn1}}/S_{\mathrm{sn2}}$, for several levels of the received power P_S.

Dividing the two PSDs (36) and (39) (and using (32)) can help to find the dominant shot noise expression

$$\frac{S_{\mathrm{sn1}}(f)}{S_{\mathrm{sn2}}(f)} = \frac{4RP_S}{qB_{\mathrm{RF}}} \qquad (40)$$

which is plotted in Fig. 3. It can be seen that, for a received power of -50 dBm and a front end bandwidth of 10 GHz, S_{n1} dominates S_{n2} by more than a factor of ten. Thus, it is safe to assume that the relevant shot noise PSD is generated by the signal $\times$ noise beat note

$$S_{\mathrm{sn}}(f) = S_{\mathrm{sn1}}(f) = \frac{(U_0 C_1 C_2 R_T G_{\mathrm{RF}})^2}{2} \cdot S_n(f). \qquad (41)$$

At significantly lower levels of P_S (or higher bandwidths B_{RF}), though, S_{sn1} and S_{sn2} are comparable in size and both expressions have to be taken into account. The assumption of the signal $\times$ noise beat note being the dominant shot noise expression will be verified in Section VI-B.

The phase-error variance due to shot noise can be calculated through

$$\sigma_{E,\mathrm{sn}}^2 = \int_0^\infty \frac{S_{\mathrm{sn}}(f)}{K_{\mathrm{PD}}^2} |H(f)|^2 df \qquad (42)$$

where, according to (21), $H(f)$ is the closed-loop transfer function of the loop. Using (20), (32), and (41) for the phase detector gain and the shot noise PSDs, and keeping in mind that, by definition

$$B_n = \int_0^\infty |H(f)|^2 df$$

and (42) becomes

$$\sigma_{E,\mathrm{sn}}^2 = \frac{qB_n}{RP_S\phi_d^2}. \qquad (43)$$

Equation (43) describes the phase-error variance in a dither loop due to photodiode shot noise. When comparing (43) with the phase-error variance due to phase dithering (27) and phase noise (30), it is interesting to note that the shot noise induced phase-error variance depends on ϕ_d and B_n in opposite directions.

D. Additional Noise Contributions

In Sections IV-A–C, the phase-error variances due to phase dithering, white frequency noise induced phase noise and shot noise have been calculated. These are not the only noise sources in a dither loop. Namely $1/f$ frequency noise (frequency flicker noise) generates considerable phase errors if it is not properly suppressed. Frequency flicker noise can be reduced with an additional pole at low frequencies in the loop filter transfer function. This has been omitted here, because it increases the computational effort without providing more insight into the loop operation. For the local oscillator intensity noise, it has been shown in [34] that a large amount of noise reduction can be achieved by using a balanced detector front end. This is at the condition of equal path lengths from the coupler output ports to the photodiodes. Lastly, thermal noise has been neglected because it is assumed that the receiver operates in shot noise limited conditions.

V. POWER PENALTIES

In the preceding Section IV, expressions for the phase-error variance due to various noise sources have been developed. It has been stated before that a nonzero phase error will reduce the SNR and therefore increase the BER. The power penalty shall be defined as the ratio of the deteriorated SNR to the SNR of an ideal (i.e., zero phase error) receiver. This section focuses on expressions for the power penalty induced by phase dithering, phase noise and shot noise.

For the analysis of the power penalty, it is assumed that, in the transmitter, the stochastic user signal is applied to an ideal phase modulator. The user signal consists of binary rectangular pulses of duration T_b. In the homodyne receiver, the detected base-band signal is deteriorated by additive white Gaussian noise. The detected signal is fed into a correlator, followed by a threshold decision circuit. The correlator is built with a matched filter, the noise bandwidth of which amounts to $1/2T_b = R_b/2$.

With this configuration, the maximally achievable SNR follows from (31) for zero phase error $(\phi_E(t) = 0)$

$$\mathrm{SNR}_{\max} = \rho_0^2 = \frac{U_0^2}{(R_T G_{\mathrm{RF}}/2)^2 S_n(f) R_b/2}. \qquad (44)$$

Using (6) and (32), (44) reduces to

$$\rho_0^2 = \frac{4RP_S}{qR_b} \qquad (45)$$

which is the formula for the SNR of optical homodyne detection [1], [11]. With the above SNR value at the input of a threshold decision circuit, it can be shown that the BER of the ideal receiver amounts to [1], [43]

$$\mathrm{BER}_0 = \frac{1}{2}\mathrm{erfc}\left(\frac{\rho_0}{\sqrt{2}}\right) = Q(\rho_0) \qquad (46)$$

where $\mathrm{erfc}(\,\cdot\,)$ denotes the complementary error function, and $Q(\,\cdot\,)$ is the Gaussian Q-function (both notations are common).

A. Phase Dither Power Penalty

For the following calculation, it is assumed that the feedback loop is only affected by phase dithering. Phase noise is switched off, and shot noise is present during data detection, but it does not flow into the phase-locking branch. This highly artificial setup leads to a closed and simplified expression for the power penalty due to LO phase dithering. A more accurate, but also more complex, expression will be presented in Section V-B.

With a nonzero phase error, the SNR at the input of the decision circuit amounts to

$$\mathrm{SNR} = \rho^2 = \frac{4RP_S \cos^2 \phi_E(t)}{qR_b} = \rho_0^2 \cos^2 \phi_E(t). \qquad (47)$$

Since phase dithering is the only perturbation on the LO phase, the total phase-error signal can be written as

$$\phi_E(t) = \phi_d \cos(\omega_d t) \qquad (48)$$

so that the SNR becomes [using the double angle formula and the series expansion (13)]

$$
\begin{aligned}
\rho_{\mathrm{dither}}^2 &= \frac{\rho_0^2}{2}(1 + \cos 2\phi_E(t)) \\
&= \frac{\rho_0^2}{2}(1 + J_0(2\phi_d) - 2J_2(2\phi_d)\cos(2\omega_d t) + \cdots) \\
&\approx \frac{\rho_0^2}{2}(1 + J_0(2\phi_d))
\end{aligned}
\qquad (49)
$$

For the last line of (49), it has been used that $J_0(z) \gg J_{2k}(z)$ for small arguments z and $k > 1, k \in \mathbf{N}$. Using the expansion

$$J_\nu(z) = (z/2)^\nu \sum_{k=0}^{\infty} \frac{(-z^2/4)^k}{k!\Gamma(\nu+k+1)} \qquad (50)$$

from [36], (49) can further be simplified to

$$\rho_{\mathrm{dither}}^2 = \frac{\rho_0^2}{2}\left(2 - \phi_d^2 + \frac{\phi_d^4}{4} - \cdots\right) \approx \rho_0^2\left(1 - \frac{\phi_d^2}{2}\right). \qquad (51)$$

Finally, the power penalty due to LO phase dithering amounts to

$$\epsilon_{\mathrm{dither}}(\phi_d) = \frac{\rho_{\mathrm{dither}}^2}{\rho_0^2} = 1 - \frac{\phi_d^2}{2} = 1 - \sigma_{E,\mathrm{dither}}^2 \qquad (52)$$

which is plotted in Fig. 4. It can be seen that the power penalty is very small for reasonable values of the phase dither amplitude ϕ_d.

The power penalty due to phase locking is a unique property of a PLL and can be used for comparison with other designs. In a balanced loop, it amounts to

$$\epsilon_{\mathrm{balanced}} = \sin^2 \phi_{\mathrm{mod}} = 1 - \cos^2 \phi_{\mathrm{mod}} \qquad (53)$$
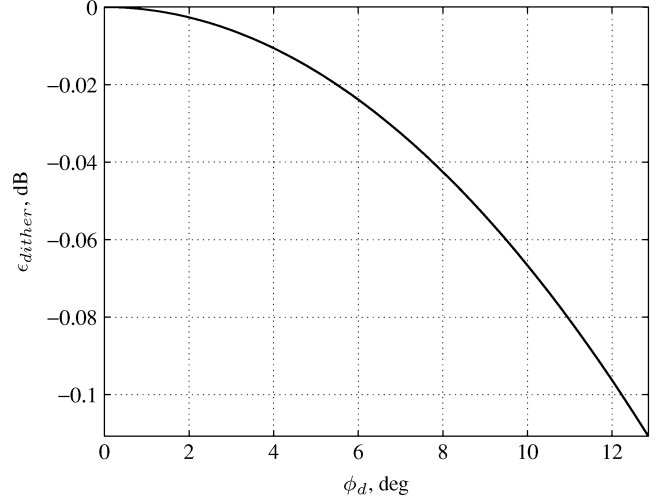

Fig. 4. Approximated power penalty due to LO phase dithering.

where ϕ_{mod} denotes the modulation depth of the optical carrier [12]. The power penalty in a Costas loop is determined by the power splitting ratio κ of the $90°$ coupler [16]

$$\epsilon_{\mathrm{Costas}} = 1 - \kappa. \qquad (54)$$

The similarity of (52), (53), and (54) supports the evaluations made thus far.

B. Overall Power Penalty

In case of a nonzero phase error, the incident BER amounts to

$$\mathrm{BER} = \frac{1}{2}\mathrm{erfc}\left(\frac{\rho_0}{\sqrt{2}}\cos\phi_E(t)\right). \qquad (55)$$

It is known from [44] that this expression can be evaluated through

$$\mathrm{BER} = \frac{1}{2}\mathrm{erfc}\left(\frac{\rho_0}{\sqrt{2}}\right) + \sum_{l=0}^{\infty}(-1)^l H_l B_l \qquad (56a)$$

with

$$H_l = \frac{\rho_0 e^{-\rho_0^2/4}}{\sqrt{2\pi}(2l+1)}\left(I_l\left(\rho_0^2/4\right) + I_{l+1}\left(\rho_0^2/4\right)\right) \qquad (56b)$$

$$B_l = 1 - \mathrm{E}[\cos((2l+1)\phi_E(t))]. \qquad (56c)$$

In (56b), $I_l(\,\cdot\,)$ denotes the modified Bessel function of the first kind of order l. It has to be recalled that, according to (9a), the total phase error $\phi_E(t)$ consists of the residual phase error $\phi_e(t)$ and the phase dither signal

$$\phi_E(t) = \phi_e(t) + \phi_d \cos(\omega_d t).$$

The residual phase error $\phi_e(t)$ is a linear combination of the phase noise and shot noise processes. These processes are presumed to be statistically independent and Gaussian distributed

with zero mean. Then, the sum process $\phi_e(t)$ has a Gaussian distribution function, zero mean, and a variance of

$$\sigma_e^2 = \sigma_{E,\mathrm{pn}}^2 + \sigma_{E,\mathrm{sn}}^2 \tag{57}$$

where $\sigma_{E,\mathrm{pn}}^2$ and $\sigma_{E,\mathrm{sn}}^2$ are determined by (30) and (43), respectively. A further property of $\phi_e(t)$, which will be used in the following calculation, is the characteristic function [42]

$$\mathrm{E}[e^{j\omega\phi_e(t)}] = e^{-\omega^2\sigma_e^2/2}. \tag{58}$$

Plugging (9a) into (56c) yields

$$B_l = 1 - \mathrm{E}[\cos\left((2l+1)(\phi_e(t) + \phi_d\cos\left(\omega_d t\right))\right)] \tag{59}$$

and transformations on the expected value result in

$$\begin{aligned}
\cos\left((2l+1)\phi_e(t) + (2l+1)\phi_d\cos\left(\omega_d t\right)\right) \\
= \cos\left((2l+1)\phi_e(t)\right) \cdot \left(J_0((2l+1)\phi_d)\right. \\
\left. - J_2((2l+1)\phi_d)\cos\left(2\omega_d t\right) + \cdots\right) \\
- \sin\left((2l+1)\phi_e(t)\right) \\
\cdot \left(J_1((2l+1)\phi_d)\cos\left(\omega_d t\right) - \ldots\right).
\end{aligned} \tag{60}$$

In (60), all $\cos\left(n\omega_d t\right)$ expressions have an expected value of zero for $n \geq 1, n \in \mathbf{N}$. Thus, (59) reduces to

$$\begin{aligned}
B_l &= 1 - J_0((2l+1)\phi_d)\mathrm{E}[\cos\left(2l+1\right)\phi_e(t)] \\
&= 1 - J_0((2l+1)\phi_d)\exp\left(-(2l+1)^2\sigma_e^2/2\right)
\end{aligned} \tag{61}$$

where the second line follows from (58) while using Euler's identity. The formulas (56a), (56b), and (61) determine the BER $\mathrm{BER}(\rho_0, \sigma_e, \phi_d)$ in a dither loop. The associated SNR amounts to

$$\mathrm{SNR} = \rho^2 = 2 \cdot (\mathrm{erfc}^{-1}(2 \cdot \mathrm{BER}(\rho_0, \sigma_e, \phi_d)))^2 \tag{62}$$

where $\mathrm{erfc}^{-1}(\cdot)$ denotes the inverse function of the complementary error function. The overall power penalty due to phase noise, shot noise and phase dithering is found to be

$$\epsilon(\rho_0, \sigma_e, \phi_d) = \frac{2 \cdot (\mathrm{erfc}^{-1}(2 \cdot \mathrm{BER}(\rho_0, \sigma_e, \phi_d)))^2}{\rho_0^2}. \tag{63}$$

An example of (63) is plotted in Fig. 5 for $\rho_0^2 = 15.6$ dB. According to (46), this SNR level is equal to a BER of 10^{-9} of the ideal (i.e., zero phase error) homodyne receiver.

With the theory derived in this section, the simplified power penalty expression (52) can be verified. This is done by evaluating (63) for a residual phase error standard deviation of zero, so that the loop is only affected by phase dithering

$$\epsilon(\rho_0, 0, \phi_d) \approx \epsilon_{\mathrm{dither}}(\phi_d). \tag{64}$$

A comparison of Figs. 4 and 5 for a power penalty value of 0.05 dB reveals a deviation of less than 2% of the two calculation methods. This is well within a reasonable accuracy range.
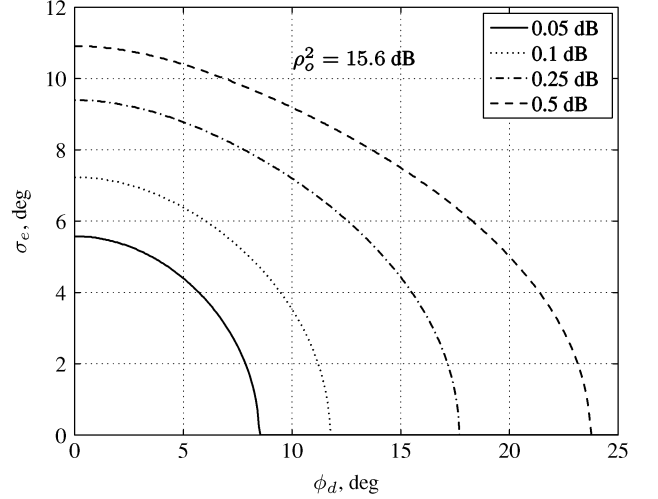

Fig. 5. Overall power penalty in a dither loop as a function of the residual phase error standard deviation σ_e and the phase dither amplitude ϕ_d.

VI. DITHER LOOP SYNTHESIS

In the preceding sections, the relevant noise expressions, their effect on the phase-error variance and the associated power penalties have been derived. This knowledge can be used to develop a design rule for an optimized loop, with minimum phase-error variance and hence, a minimum power penalty due to incomplete carrier phase recovery. The two main design parameters are the phase dither amplitude ϕ_d and the loop noise bandwidth B_n.

A. Phase Error Minimization

According to the central-limit theorem [42], the total phase-error variance is the sum of the variances of the individual noise sources [(27), (30), and (43)]

$$\begin{aligned}
\sigma_E^2 &= \sigma_{E,\mathrm{dither}}^2 + \sigma_{E,\mathrm{pn}}^2 + \sigma_{E,\mathrm{sn}}^2 \\
\sigma_E^2(\phi_d, B_n) &= \frac{\phi_d^2}{2} + \frac{3\pi\Delta\nu}{4B_n} + \frac{qB_n}{RP_S\phi_d^2}.
\end{aligned} \tag{65}$$

This holds true only if the noise processes are statistically independent, which can be safely assumed in a dither loop. Calculating the partial derivatives $\partial\sigma_E^2/\partial\phi_d$ and $\partial\sigma_E^2/\partial B_n$, and solving for the roots, yields

$$B_{n,\mathrm{opt}} = \frac{1}{2}\left(\frac{(3\pi)^2 RP_S\Delta\nu^2}{q}\right)^{1/3} \tag{66a}$$

$$\phi_{d,\mathrm{opt}} = \left(\frac{3\pi q\Delta\nu}{RP_S}\right)^{1/6}. \tag{66b}$$

These values define the global minimum of the total phase-error variance ϕ_E^2. Evaluating the optimal values (66) in the variances (27), (30), and (43), yields

$$\sigma_{E,\mathrm{dither}}^2 = \sigma_{E,\mathrm{pn}}^2 = \sigma_{E,\mathrm{sn}}^2 = \frac{1}{2}\left(\frac{3\pi q\Delta\nu}{RP_S}\right)^{1/3} \tag{67}$$
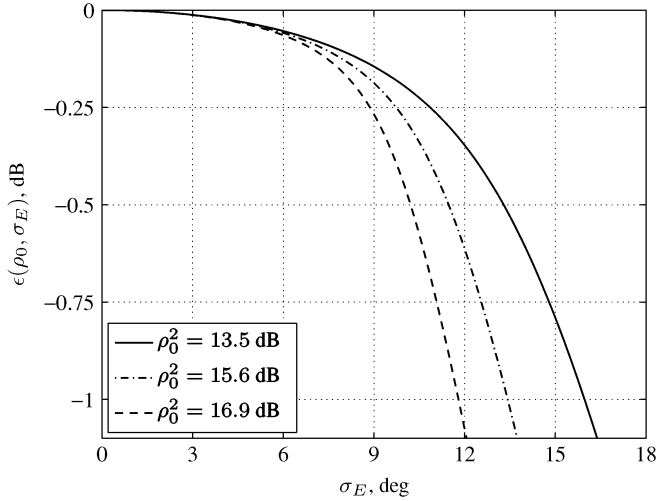
Fig. 6. Overall power penalty $\epsilon(\rho_0, \sigma_E)$ in an optimally designed dither loop. The SNR values ρ_0^2 of 13.5, 15.6, and 16.9 dB lead to BERs of 10^{-6}, 10^{-9}, and 10^{-12}, respectively.

Fig. 7. Phase error standard deviation σ_E as a function of the BRLR in an optimally designed dither loop.

so that each of the three expressions in (65) contribute the same amount of phase-error variance. The total phase-error variance becomes

$$\sigma_E^2 = \frac{3}{2}\left(\frac{3\pi q \Delta\nu}{RP_S}\right)^{1/3} \tag{68}$$

and the variance due to the residual phase error $\phi_e(t)$ can be written as

$$\sigma_e^2 = \sigma_{E,\mathrm{pn}}^2 + \sigma_{E,\mathrm{sn}}^2 = 2\sigma_{E,\mathrm{dither}}^2 = \phi_d^2. \tag{69}$$

It has been shown in Section V-B how to compute the power penalty in a dither loop for an arbitrary combination of ϕ_d and σ_e. With (69), ϕ_d and σ_e are in a fixed relation, so that the power penalty can be calculated as a function of the phase error standard deviation σ_E alone

$$\epsilon(\rho_0, \sigma_e, \phi_d) \rightarrow \epsilon(\rho_0, \sigma_E). \tag{70}$$

This can be done by changing (61) to

$$B_l = 1 - J_0(\sqrt{2/3} \cdot (2l+1)\sigma_E)\exp\left(-2(2l+1)^2\sigma_E^2/6\right) \tag{71}$$

or by reading the power penalty value from Fig. 5 for $\sigma_e = \phi_d$. An example of (70) is depicted in Fig. 6.

B. Dither Loop Design Rule

The coherent receiver has two distinct requirements on the received power P_S. It follows from (68) that the phase-locking branch demands an optical power (at the receiver input) of
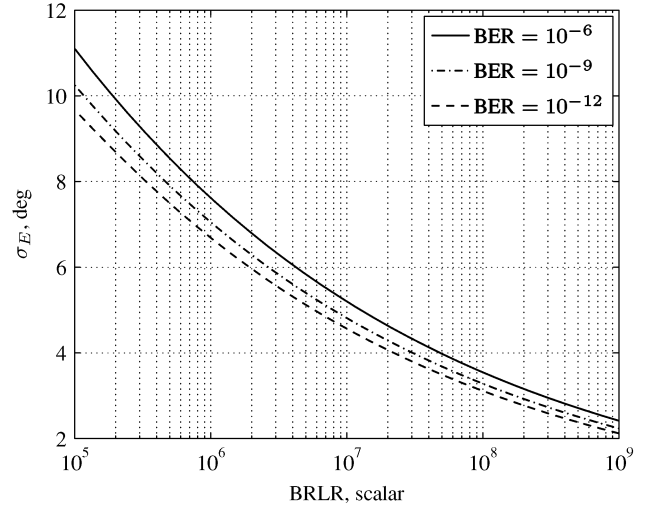
$$P_S = \frac{81\pi q \Delta\nu}{8R\sigma_E^6} \tag{72}$$

for specified values of the laser linewidth $\Delta\nu$ and the acceptable phase error standard deviation σ_E. The power requirement of the data-detection branch can be calculated through

$$\mathrm{BER} = \frac{1}{2}\mathrm{erfc}\left(\sqrt{\frac{\rho_0^2\epsilon}{2}}\right) = \frac{1}{2}\mathrm{erfc}\left(\sqrt{\frac{2RP_S\epsilon}{qR_b}}\right) \tag{73a}$$

$$\rightarrow P_S = \frac{qR_b}{2R\epsilon}(\mathrm{erfc}^{-1}(2 \cdot \mathrm{BER}))^2 \tag{73b}$$

for given values of R_b, BER and the acceptable power penalty ϵ. The receiver reaches its optimum operating condition when both power requirements (72) and (73b) are equal. This leads to the computation of the optimum phase error standard deviation σ_E for given values of $R_b, \Delta\nu$ and BER

$$\sigma_{E,\mathrm{opt}} = \left(\frac{81\pi\epsilon_{\mathrm{opt}}}{4 \cdot \mathrm{BRLR}}\right)^{1/6}(\mathrm{erfc}^{-1}(2 \cdot \mathrm{BER}))^{-1/3} \tag{74}$$

where

$$\mathrm{BRLR} = \frac{R_b}{\Delta\nu} \tag{75}$$

is the dimensionless bit-rate-to-linewidth ratio (BRLR).[1] It is important to note that (74) cannot be solved explicitly, because the computation of ϵ through (70), (63), (56a), (56b), and (71) does not have an inverse function. An iterative algorithm to solve (74) is presented in the Appendix. An example of (74) is shown in Fig. 7.

The theory derived until here describes a complete design rule for a dither loop, based on specified values of $R_b, R, \Delta\nu$ and BER. The phase error standard deviation σ_E and the power penalty ϵ follow from (74), through the algorithm described in the Appendix. The required power P_S can be calculated with (72) or (73b) (both equations yield the same value). Equations

---

[1]The BRLR should not be confused with the spectral efficiency of coding theory. It is merely an indication for the receiving conditions, under which the system is operating. High values of the BRLR lead to small phase errors, and consequently, to low power penalties.

TABLE II
OPTIMUM DITHER LOOP DESIGNS FOR TWO LASER TYPES AND THREE DIFFERENT VALUES OF THE SYSTEM BIT RATE

Parameter	Symbol	Unit	Value					
Bit error rate	BER	scalar	10^{-9}					
Quantum efficiency	η	scalar	0.75					
Laser type			Nd:YAG			Fiber laser, ECL		
Wavelength	λ	nm	1064			1550		
Linewidth	$\Delta\nu$	Hz	10			$1 \cdot 10^4$		
Responsivity	R	A/W	0.64			0.94		
System bit rate	R_b	GHz	1	5	10	1	5	10
Bit-rate-to-linewidth ratio	BRLR	scalar	10^8	$5 \cdot 10^8$	10^9	10^5	$5 \cdot 10^5$	10^6
Phase error std. dev.	σ_E	deg	3.3	2.5	2.2	10.2	7.9	7.0
Power penalty	ϵ	dB	-0.02	-0.009	-0.007	-0.34	-0.12	-0.09
Required power	P_S	dBm	-56.5	-49.5	-46.5	-57.8	-51.0	-48.0
Loop noise bandwidth	B_n	kHz	21.6	36.8	46.4	2210	3720	4670
Phase dither amplitude	ϕ_d	deg	2.7	2.0	1.8	8.4	6.5	5.8
Natural frequency ($\zeta = 1/\sqrt{2}$)	f_n	kHz	6.5	11.1	13.9	663	1120	1400
Dither frequency	f_d	kHz	65	111	139	6630	11200	14000

(66a) and (66b) determine the optimum loop noise bandwidth B_n and phase dither amplitude ϕ_d. Choosing a damping factor ζ and solving (24c) yields the natural frequency of the loop f_n. The dither frequency f_d has to be chosen much larger than f_n, e.g., $f_d = 10 \cdot f_n$.

As an example, several dither loop designs with optimum performance measures are presented in Table II. For all six designs, the overall power penalty due to the phase error $\phi_E(t)$ remains very low. This is because with the specified values of R_b and $\Delta\nu$, the power demand is determined by the data-detection unit, and not by the phase-locking branch. Moreover, it is interesting to note that the system with the smaller laser linewidth requires higher optical input powers, because of an inferior photodiode responsivity. The advantage of the narrow-linewidth system lies in much smaller values of the optimum noise bandwidth, which eases the design of the feedback loop.

During the analysis, various assumptions have been made to simplify the mathematics. For the linearized loop model, it has been stated that the phase error standard deviation should not exceed $10°$. It can bee seen in Table II that this is achieved for all loops. The system with the smallest bit-rate-to-linewidth ratio is at the limit of the allowed phase error standard deviation. A further assumption has been made during the calculation of the relevant shot noise contribution. It has been found in Section IV-C that the signal × noise beat note exceeds the noise × noise beat note by at least a factor of ten for most receiver setups. Reading the values of R_b and P_S from Table II and comparing them with Fig. 3 (where $R_b \approx B_{RF}$), reveals that the signal × noise beat note is indeed the dominant shot noise expression.

VII. CONCLUSION

To achieve the highest possible sensitivity in an optical transmission system without coding, it is inevitable to use homodyne detection. Homodyning requires an OPLL, for which the dither loop represents a possible design. Compared to other designs, the dither loop is advantageous due to the residual-carrier free transmission and a lower technological complexity in the optical signal path (180°/3-dB hybrid instead of an asymmetric 90° coupler). The dither loop imposes only one restriction on the user signal, which is a constant envelope. Furthermore, the

amount of power which is fed to the phase-locking branch can be adaptively controlled within the receiver by changing the phase dither amplitude ϕ_d.

In this paper, the dither loop has been investigated theoretically for the first time. An expression for the phase detector gain K_{PD} has been extracted. The effect of phase dithering, white frequency noise induced phase noise and shot noise on the phase-error variance is analyzed. For comparison with other OPLL types, a simplified expression for the power penalty due to phase dithering has been calculated. In a more complex evaluation, the overall power penalty due to phase dithering and the residual phase error is found. The knowledge of the phase-error variances due to the individual noise sources is used to compute values of ϕ_d and B_n that minimize the total phase-error variance. Finally, this led to the development of a design rule for dither loops with optimum performance measures, i.e., minimized power requirements and minimum power penalties due to phase locking.

APPENDIX
ITERATIVE COMPUTATION OF σ_E AND ϵ

Equation (74) for σ_E cannot be solved analytically, because the power penalty ϵ depends on σ_E through (70), (63), (56a), (56b), and (71). This dependency can not be inverted. The following iterative algorithm is proposed to compute σ_E for given values of R_b, $\Delta\nu$ and BER.

1) Choose an ϵ_1 which is expected to be smaller than the true power penalty ϵ, i.e.,

$$\epsilon_1 < \epsilon.$$

As it can be seen from Table II, the power penalties are usually very small. A good choice for ϵ_1 could therefore be a power penalty of 0.89 (-0.5 dB).

2) Solve (74)

$$\sigma_{E,n} = \left(\frac{81\pi\epsilon_{1,n}}{4 \cdot \text{BRLR}} \right)^{1/6} (\text{erfc}^{-1}(2 \cdot \text{BER}))^{-1/3}.$$

Here, $\epsilon_{1,n}$ and $\sigma_{E,n}$ denote ϵ_1 and σ_E of the nth iteration, respectively.

3) Calculate the SNR ρ_0^2 of the ideal receiver [i.e., from (73a)]

$$\rho_{0,n}^2 = \frac{(\text{erfc}^{-1}(2 \cdot \text{BER}))^2}{\epsilon_{1,n}}.$$

4) Compute the power penalty ϵ_2 through (70), (63), (56a), (56b), and (71) for the given combination of $\sigma_{E,n}$ and $\rho_{0,n}$

$$\epsilon_{2,n} = \epsilon(\rho_{0,n}, \sigma_{E,n}).$$

With a good choice in step 1), $\epsilon_{2,n}$ is larger than $\epsilon_{1,n}$.

5) Calculate a new ϵ_1 between $\epsilon_{1,n}$ and $\epsilon_{2,n}$

$$\epsilon_{1,n+1} = \frac{\epsilon_{1,n} + \epsilon_{2,n}}{2}.$$

6) Repeat with step 2). A termination condition can be defined as

$$\frac{|\epsilon_{2,n} - \epsilon_{1,n}|}{\epsilon_{1,n}} < 10^{-6}$$

or any other level of the desired accuracy.

When the algorithm terminates, $\epsilon_{1,n}$, and $\sigma_{E,n}$ contain values of ϵ and σ_E that solve (74) with a sufficiently good accuracy, under consideration of the dependency of ϵ from σ_E through (70), (63), (56a), (56b), and (71).

REFERENCES

[1] J. R. Barry and E. A. Lee, "Performance of coherent optical receivers," *Proc. IEEE*, vol. 78, no. 8, pp. 1369–1394, Aug. 1990.

[2] J. Salz, "Modulation and detection for coherent lightwave communications," *IEEE Commun. Mag.*, vol. 24, no. 6, pp. 38–49, Jun. 1986.

[3] V. W. S. Chan, "Space coherent communication systems—An introduction," *J. Lightw. Technol.*, vol. LT-5, no. 4, pp. 633–637, Apr. 1987.

[4] T. Okoshi and K. Kikuchi, *Coherent optical fiber communications*. Tokyo, Japan: KTK Scientific, 1988.

[5] G. P. Agrawal, *Fiber-Optic Communication Systems*, 3rd ed. New York: Wiley, 2002.

[6] W. R. Leeb, "Degradation of signal to noise ratio in optical free space data links due to background illumination," *Appl. Opt.*, vol. 28, no. 15, pp. 3443–3449, Aug. 1989.

[7] R. F. Kalman, J. C. Fan, and L. G. Kazovsky, "Dynamic range of coherent analog fiber-optic links," *J. Lightw. Technol.*, vol. 12, no. 7, pp. 1263–1277, Jul. 1994.

[8] A. H. Gnauck, K. C. Reichmann, J. M. Kahn, S. K. Korotky, J. J. Veselka, and T. L. Koch, "4-Gb/s Heterodyne transmission experiments using ASK, FSK, and DPSK modulation," *IEEE Photon. Technol. Lett.*, vol. 2, no. 12, pp. 908–910, Dec. 1990.

[9] K. Kudielka and K. Pribil, "Transparent optical intersatellite link using double-sideband modulation and homodyne reception," *Int. J. Electron. Commun.*, vol. 56, no. 4, pp. 254–260, 2002.

[10] S. D. Personick, "An image band interpretation of optical heterodyne noise," *Bell Syst. Tech. J.*, vol. 50, no. 1, pp. 213–216, Jan. 1971.

[11] L. G. Kazovsky, "Optical heterodyning versus optical homodyning: A comparison," *J. Opt. Commun.*, vol. 6, no. 1, pp. 18–24, Mar. 1985.

[12] ——, "Balanced phase-locked loops for optical homodyne receivers: Performance analysis, design considerations, and laser linewidth requirements," *J. Lightw. Technol.*, vol. LT-4, no. 2, pp. 182–195, Feb. 1986.

[13] J. M. Kahn, "1 Gbit/s PSK homodyne transmission system using phase-locked semiconductor lasers," *IEEE Photon. Technol. Lett.*, vol. 1, no. 10, pp. 340–342, Oct. 1989.

[14] L. G. Kazovsky and D. A. Atlas, "A 1320-nm experimental optical phase-locked loop: Performance investigation and PSK homodyne experiments at 140 Mb/s and 2 Gb/s," *J. Lightw. Technol.*, vol. 8, no. 9, pp. 1414–1425, Sep. 1990.

[15] J. M. Kahn, A. H. Gnauck, J. J. Veselka, and S. K. Korotky, "4-Gb/s PSK homodyne transmission system using phase-locked semiconductor lasers," *IEEE Photon. Technol. Lett.*, vol. 2, no. 4, pp. 285–287, Apr. 1990.

[16] L. G. Kazovsky, "Decision-driven phase-locked loop for optical homodyne receivers: Performance analysis and laser linewidth requirements," *J. Lightw. Technol.*, vol. LT-3, no. 6, pp. 1238–1247, Dec. 1985.

[17] S. Norimatsu and K. Iwashita, "10 Gbit/s optical PSK homodyne transmission experiments using external cavity DFB LDs," *Electron. Lett.*, vol. 26, no. 10, pp. 648–649, May 1990.

[18] D. F. Hornbachner, M. A. Schreiblehner, W. R. Leeb, and A. L. Scholtz, "Experimental determination of power penalty contributions in an optical Costas-type phase-locked loop receiver," in *Proc. SPIE Free-Space Laser Communication Technologies TV*, Jan. 1992, vol. 1635, pp. 10–18.

[19] S. Norimatsu, K. Iwashita, and K. Noguchi, "An 8 Gb/s QPSK optical homodyne detection experiment using external-cavity laser diodes," *IEEE Photon. Technol Lett.*, vol. 4, no. 7, pp. 765–767, Jul. 1992.

[20] S. Norimatsu, H. Mawatari, Y. Yoshikuni, O. Ishida, and K. Iwashita, "10 Gbit/s optical BPSK homodyne detection experiment with solitary DFB laser diodes," *Electron. Lett.*, vol. 31, no. 2, pp. 125–127, Jan. 1995.

[21] B. Wandernoth, "20 Photons/bit 565 Mbit/s PSK homodyne receiver using synchronisation bits," *Electron. Lett.*, vol. 28, no. 4, pp. 387–388, Feb. 1992.

[22] W. Glatt, M. A. Schreiblehner, C. Haider, and W. R. Leeb, "Optical PSK homodyne system using a switched residual carrier for phase synchronisation," *Electron. Lett.*, vol. 32, no. 15, pp. 1386–1387, Jul. 1996.

[23] C. Rapp, "Modulated residual carrier method with envelope processing: A novel phase synchronisation method for optical homodyne transmission," *J. Commun. Res. Lab.*, vol. 46, no. 3, pp. 321–323, Nov. 1999.

[24] K. Kudielka and W. Klaus, "Optical homodyne PSK receiver: Phase synchronization by maximizing base-band signal power," in *Proc. IEEE LEOS'99*, San Francisco, CA, Nov. 1999, vol. 1, pp. 295–296.

[25] F. Herzog, K. Kudielka, D. Erni, and W. Bachtold, "Optical phase-locked loop for transparent inter-satellite communications," *Opt. Exp.*, vol. 13, no. 10, pp. 3816–3822, May 2005.

[26] W. R. Leeb, "Realization of 90°- and 180° Hybrids for Optical Frequencies," *Int. J. Electron. Commun.*, vol. 37, no. 5/6, pp. 203–206, 1983.

[27] L. G. Kazovsky, L. Curtis, W. C. Young, and N. K. Cheung, "All-fiber 90° optical hybrid for coherent communications," *Appl. Opt.*, vol. 26, no. 3, pp. 437–439, Feb. 1987.

[28] Y. Wang and W. R. Leeb, "A 90° fiber hybrid for optimal signal power utilization," *Appl. Opt.*, vol. 26, no. 19, pp. 4181–4184, Oct. 1987.

[29] W. R. Leeb, "Optical 90° hybrid for costas-type receivers," *Electron. Lett.*, vol. 26, no. 18, pp. 1431–1432, Aug. 1990.

[30] R. Garreis, "90° optical hybrid for coherent receivers," in *Proc. SPIE Opt. Space Commun.II*, Munich, Germany, Jun. 1991, vol. 1522, pp. 210–219.

[31] R. Montgomery and R. DeSalvo, "A novel technique for double sideband suppressed carrier modulation of optical fields," *IEEE Photon. Technol Lett.*, vol. 7, no. 4, pp. 434–436, Apr. 1995.

[32] J. M. Kahn, B. L. Kasper, and K. J. Pollock, "Optical phaselock receiver with multigigahertz signal bandwidth," *Electron. Lett.*, vol. 25, no. 10, pp. 626–628, May 1989.

[33] K. Pribil, C. Serbe, B. Wandernoth, and C. Rapp, "SOLACOS YKS: An optical high datarate communication system for intersatellite link applications," in *Proc. SPIE Free-Space Laser Communication Technologies VII*, San Jose, CA, Feb. 7–8, 1995, vol. 2381, pp. 83–88.

[34] G. L. Abbas, V. W. S. Chan, and T. K. Yee, "Local-oscillator excess-noise suppression for homodyne and heterodyne detection," *Opt. Lett.*, vol. 8, no. 8, pp. 419–421, Aug. 1983.

[35] F. M. Gardner, *Phaselock Techniques*. New York: Wiley, 1966.

[36] M. Abramowitz and I. A. Stegun, Eds., *Handbook of Mathematical Functions with Formulas, Graphs, and Mathematical Tables*. New York: Dover, 1972.

[37] S. K. Nielsen, B. F. Skipper, and J. P. Villadsen, "Universal AFC for use in optical DPSK systems," *Electron. Lett.*, vol. 29, no. 16, pp. 1445–1446, Aug. 1993.

[38] E. A. Swanson, J. C. Livas, and R. S. Bondurant, "High sensitivity optically preamplified direct detection DPSK receiver with active delay-line stabilization," *IEEE Photon. Technol. Lett.*, vol. 6, no. 2, pp. 263–265, Feb. 1994.

[39] R. E. Best, *Phase-Locked Loops: Design, Simulation and Applications*. New York: McGraw-Hill, 1997.

[40] J. J. Spilker, *Digital Communications by Satellite*. Englewood Cliffs, NJ: Prentice-Hall, 1977.

[41] S. Haykin, *Communication Systems*, 4th ed. New York: Wiley, 2001.

[42] A. Papoulis, *Probability, Random Variables, and Stochastic Processes*. New York: McGraw-Hill, 1965.

[43] J. G. Proakis, *Digital Communications*, 3rd ed. New York: McGraw-Hill, 1995.

[44] V. K. Prabhu, "PSK performance with imperfect carrier phase recovery," *IEEE Trans. Aerosp. Electron. Syst.*, vol. AES-12, no. 2, pp. 275–286, Mar. 1976.

Frank Herzog (S'02–M'05) was born in Münsterlingen, Switzerland, in 1975. He received the M.S. degree (Dipl. El.-Ing.) in electrical engineering and the Ph.D. degree from the Swiss Federal Institute of Technology (ETH), Zurich, Switzerland, in 2001 and 2006, respectively. He received the Ph.D. degree for his work on optical space communication terminals, which he conducted in the framework of a collaboration of ETH, Contraves Space AG, Zurich, Switzerland, and the Swiss Innovation Promotion Agency.

His research interests are in microwave electronics, optoelectronics, and optics.

Klaus Kudielka was born 1968 in Southampton, U.K. He received the M.S. degree (Dipl.-Ing.) and the Ph.D. degree (Dr. techn.) from Vienna University of Technology, Vienna, Austria, in 1992 and 1997, respectively.

From 1992 to 2000, he was an Assistant at the Institut für Nachrichtentechnik und Hochfrequenztechnik, Vienna University of Technology, specializing in free-space laser communications. From 1998 to 1999, he was a Researcher at the Communications Research Laboratory, Ministry of Posts and Telecommunications, Tokyo, Japan. Since October 2000, he has been with Contraves Space in Zurich, Switzerland.

Daniel Erni (S'88–M'93) was born in Lugano, Switzerland, in 1961. He received the El.-Ing. degree in electrical engineering from Interkantonales Technikum Rapperswil HTL, Rapperswil, Switzerland, in 1986, the Dipl. El.-Ing. degree in electrical engineering, and the Ph.D. degree from the Swiss Federal Institute of Technology (ETH), Zurich, Switzerland, in 1990 and 1996, respectively. He received the Ph.D. degree for the investigation of nonperiodic waveguide gratings and nonperiodic coupled cavity laser concepts.

Since 1990, he has been with the Laboratory for Electromagnetic Fields and Microwave Electronics, ETH, working on nonlinear wave propagation, laser diode modeling (multisection DFB and DBR lasers, VCSELs), computational electromagnetics, and on the design of nonperiodic optical waveguide gratings, e.g., by means of evolutionary algorithms. His current research interests include highly multimode optical signal transmission in optical interconnects (i.e., in optical backplanes with extremely large waveguide cross-sections) as well as alternative waveguiding concepts for dense integrated optical devices like, e.g., photonic crystal devices, couplers, and WDM filter structures. He is the Head of the Communication Photonics Group at ETH Zurich.

Dr. Erni is a member of the Swiss Physical Society, the German Physical Society, and the Optical Society of America (OSA). In 2001, he was been awarded the 2000 Outstanding Journal Paper Award by the Applied Computational Electromagnetics Society for a contribution on the application of evolutionary optimization algorithms in computational optics.

Werner Bächtold (M'71–SM'99–F'00) received the diploma and Ph.D. degree in electrical engineering from the Swiss Federal Institute of Technology (ETH), Zurich, Switzerland, in 1964 and 1968, respectively.

From 1969 to 1987, he was with the IBM Zurich Research Laboratory. He contributed to the development of the gallium–arsenide MESFET technology. In particular, he investigated the microwave noise properties and demonstrated the first *X* and *Ku*-band MESFET amplifiers. In the area of superconducting devices and circuits, he designed logic and memory circuits with Josephson junctions. He demonstrated the first nonlatching Josephson logic circuit. In a project on semiconductor lasers for digital communication, he contributed in laser modeling and design. He had several assignments at the IBM T.J. Watson Research Center, Yorktown Heights, NY. In 1987, he became Professor of electrical engineering at ETH. Until his retirement in 2005, he was Head of the Microwave Electronics Group at the Laboratory for Electromagnetic Fields and Microwave Electronics. He has taught on subjects of microwave techniques and electronics.